Elastic and inelastic scattering of 0.8 GeV protons from ^{20}Ne and ^{22}Ne

G. S. Blanpied and B. G. Ritchie*
University of South Carolina, Columbia, South Carolina 29208

M. L. Barlett, R. W. Fergerson,† G. W. Hoffmann, and J. A. McGill‡
University of Texas, Austin, Texas 78712

B. H. Wildenthal
University of New Mexico, Albuquerque, New Mexico 87131
(Received 22 October 1987)

Angular distributions for the elastic and inelastic scattering of 0.8 GeV protons from ^{20}Ne and ^{22}Ne are presented. Cross sections for protons exciting states up to about 14 MeV were measured using a high resolution spectrometer. Coupled-channels analyses of scattering cross sections for the 0^+, 2^+, 4^+, and 6^+ states in the ground-state rotational band, possible 2^-, 3^-, and 5^- members of a $K^\pi=2^-$ octupole band, and possible 1^-, 3^-, and 5^- members of a $K^\pi=0^-$ octupole band in ^{20}Ne were performed. Also reported are coupled-channels analyses of the experimental angular distributions in ^{22}Ne for the 0^+, 2^+, and 4^+ states in the ground-state band, the $K^\pi=2^+$ γ-vibrational band members, and the 2^- and 3^- members of a $K^\pi=2^-$ octupole band. Deformation parameters for states not in the ground-state rotational bands are obtained from a distorted-wave Born approximation analysis of these data. Multipole moments inferred from the deformed optical potentials are compared with moments obtained with electromagnetic measurements, low-energy proton, deuteron, ^{3}He, and ^{4}He scattering, and shell-model calculations.

I. INTRODUCTION

In several recent publications,[1-7] coupled-channels (CC) analyses of $\sim$1-GeV proton inelastic scattering from *s-d* shell nuclei and heavy rare-earth nuclei have been generally informative. These rotational-model calculations provide an excellent description of the data for the lowest 0^+, 2^+, and 4^+ states in ^{24,26}Mg and ^{20}Ne.[6,7] The large hexadecapole deformation of ^{20}Ne was also confirmed. The data for the states in the γ-vibrational bands and in the negative-parity vibrational bands of ^{24,26}Mg are also explained. To improve the knowledge of deformations in *s-d* shell nuclei and further study intermediate-energy proton inelastic scattering from light, deformed nuclei, new data for ^{20,22}Ne(p,p') at 0.8 GeV were acquired and are presented here. The data include angular distributions for excitation of the 0^+ ground state and the $(1.63,2^+)$, $(4.25,4^+)$, $(4.97,2^-)$, $(5.62,3^-)$, $(5.78,1^-)$, $(7.17,3^-)$, $(8.45,5^-)$, and $(8.7,6^+ + 1^-)$ states in ^{20}Ne and the ground state, $(1.27,2^+)$, $(3.36,4^+)$, $(4.46,2^+)$, $(5.15,2^-)$, $(5.91,3^-)$, and $(6.34,4^+)$ states in ^{22}Ne.[8]

II. EXPERIMENTAL PROCEDURE

The data were obtained using the high resolution spectrometer (HRS) of the Los Alamos Clinton P. Anderson Meson Physics Facility (LAMPF). The experimental details, including the design of the gas target, are the same as in Ref. 7. The gases were isotopically enriched to 99.95% for ^{20}Ne and 99% for ^{22}Ne.

Data were acquired for ^{20}Ne, ^{22}Ne, and ^{14}N using a gas target of identical geometry and were compared to the data of Ref. 7. The energy resolution ($\Delta E \sim 140$ keV) allowed the extraction of many peak areas from the spectra. Three spectra for ^{22}Ne(p,p'), each covering an angular range of 1.5°, are shown in Fig. 1. The resulting angular distributions are presented in Figs. 2–7. A complete tabulation of the numerical data is on deposit in PAPS.[9]

III. ^{20}Ne

In this section the results of analyzing most of the ^{20}Ne(p,p') data are presented. As in previous studies in this series,[6,7] a deformed optical potential $V(\mathbf{r})$ was determined by fitting the scattering data for the ground-state rotational band using the CC formalism, in which multistep processes are included. Then, the multipole moments of the matter density[7] were obtained from those of the optical potential. The moments obtained from the optical potential have been found to agree well with those obtained from electron scattering, Coulomb excitation, and theory.[5,7]

The CC calculation from which the deformed optical potential is obtained was performed using a version of the program JUPITER.[10] This version has been modified to include relativistic kinematics, intrinsic β_6 deformation, coupling potentials with $\Delta l=2$, 4, 6, and 8, and direct $\Delta l=4$ coupling between the ground and γ-vibrational bands.[1-4] The geometry of the optical potential is the usual Fermi form, where the radius parameter $R(\theta',\phi')$ is

$$R(\theta',\phi')=R_0\left[1+\sum_{\lambda\mu}\alpha_{\lambda\mu}Y_{\lambda\mu}(\theta',\phi')\right],$$

 ©1988 The American Physical Society

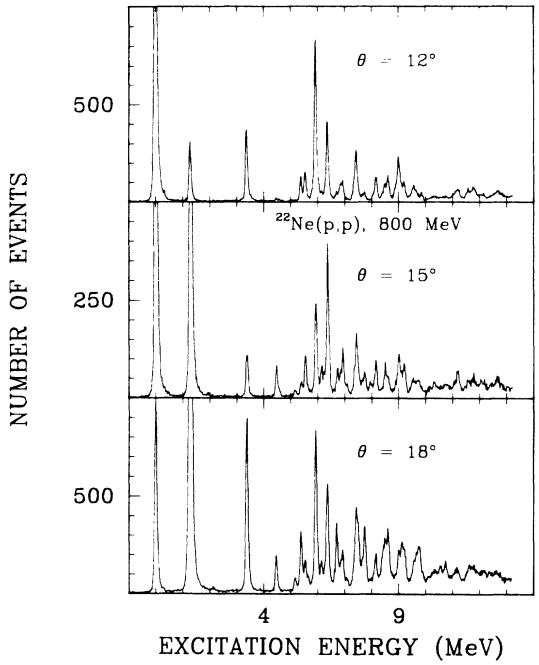

FIG. 1. Three spectra, each covering an angular range of 1.5°, for ^{22}Ne(p,p') at 0.8 GeV and $\theta_{lab}=12°$, 15°, and 18°.

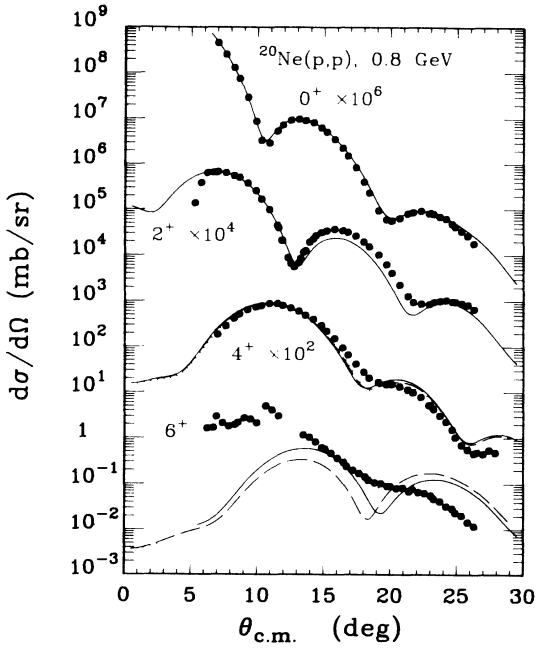

FIG. 2. Angular distributions of ^{20}Ne(p,p') at 0.8 GeV, for the 0^+, 2^+, 4^+, and unresolved doublet (1^-,6^+) states are shown. The curves result from CC calculations discussed in the text. The solid lines result from $\beta_6=+0.03$, the dashed lines from $\beta_6=0$, and the dotted lines from $\beta_6=-0.03$.

where primes denote the body-fixed coordinate system. The deformed optical potential is treated using the Legendre polynomial expansion method discussed by Tamura.[10]

Other rotational bands which are built on intrinsic vibrational states are calculated by including the appropriate vibrational terms in $R(\theta',\phi')$, so as to couple the ground-state band to the "vibrational" bands. The states in the γ band (of ^{22}Ne) were assumed to correspond to so-called γ vibrations, in which the nucleus retains the same spheroidal equilibrium deformation, but in addition oscillates such that ellipsoidal shapes are produced (the $K^\pi=2^+$ band). The observed odd-parity states were assumed to belong to an octupole vibrational band with $K^\pi=0^-$ ($J^\pi=1^-,3^-,5^-\ldots$) or with $K^\pi=2^-$ ($J^\pi=2^-,3^-,4^-,5^-\ldots$).

A. Ground-state rotational band (GSRB)

Calculations were performed for the (ground state, 0^+), ($1.63,2^+$), ($4.25,4^+$), and ($8.7,6^+$) states, with couplings and deformation up to β_6. The results reported earlier[7] are presented as the solid line in Fig. 2. The small spin-orbit potential utilized in Ref. 7 has been omitted here. The geometry of the small real central term has been fixed to that of the dominant imaginary term. The Woods-Saxon potential parameters (V, W, r, a, and r_c) are (−5.0 and 48.0 MeV and 1.06, 0.46, and 1.05 fm), while the deformation parameters (β_2, β_4, and β_6) are [+0.46, +0.27, and +0.03 (solid line)]. The dashed (dotted) line for the 6^+ state utilizes $\beta_6=0.0$ (−0.03). As mentioned in Ref. 7, the 6^+ state is unresolved from a nearby 1^- state and thus it is difficult to make a quantitative evaluation of the β_6 deformation. Varying β_6 between ±0.03 has no observable effect on the predictions for the 0^+, 2^+, and 4^+ angular distributions. We consider a value of $\beta_6=+0.03$ as a reasonable upper limit. The observed cross-section data for the 0^+, 2^+ and 4^+ states are reproduced quite well by the CC calculation, while DWBA calculations were found to give significantly poorer results.[7] Both the large cross section for the 4^+ state and the position of the first minimum in the angular distribution for the 2^+ state are evidence of a large hexadecapole deformation for the ^{20}Ne ground state.

B. $K^\pi=2^-$ octupole band

A CC calculation in which the 0^+, 2^+, and 4^+ states of the GSRB were coupled to an octupole vibrational band with $K^\pi=2^-$ is shown in Fig. 3 along with the measured angular distributions for excitation of the (4.97 MeV, 2^-), ($5.62,3^-$), and ($8.45,5^-$) states. The ($7.00,4^-$) state was not observed. The only term in the CC calculations providing the coupling between the $K=0^+$ and $K=2^-$ bands has the structure $[\alpha_{32}(Y_{32}+Y_{3-2})]$. Thus in these calculations the 2^- state is excited only by transitions which involve at least two steps, and not from the ground state directly. The 5^- state can be excited by terms in the multipole expansion of the deformation such as $Y_3\times Y_2$. A calculation using $\alpha_{32}R=1.35$ fm gives the correct slope and roughly the correct magnitude for all three states, but predicts sharper diffraction patterns than are measured.

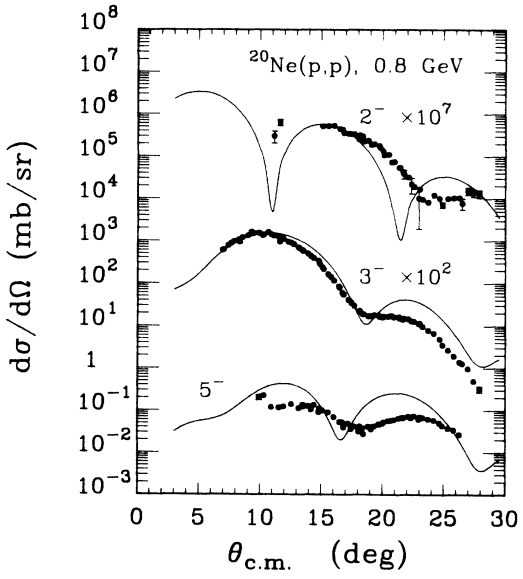

FIG. 3. Angular distributions and CC calculations for a $K^\pi=2^-$ in ^{20}Ne.

C. $K^\pi=0^-$ octupole band

The results of a CC calculation in which the first three states of the GSRB are coupled to a band with $K^\pi=0^-$ are shown in Fig. 4, along with measurements for the (5.78,1^-), (7.17,3^-), and (8.45,5^-) states. Here $\alpha_{30}R=0.60$ fm. A DWBA calculation for the 3^- state (not shown) is inferior to the CC result, predicting the first minimum 2° farther out in angle (18°) than the CC result. The disagreement between the CC result and the data for the 1^- state may possibly be due to the improper treatment in the program JUPITER of the center of mass motion in the transition potential for the 1^- state. It may also indicate that an extra direct step from the ground state, which has not been included here, may be necessary. The use of an isoscalar dipole form factor has been discussed by Put and Harakeh.[11] The fit to the 5^- state is slightly worse than was obtained with the calculation above, in which it was assumed to belong to the $K^\pi=2^-$ band. Since both calculations predict cross sections roughly equal in magnitude to the data but fail to reproduce the actual angular distribution, the true nature of the 5^- state is not revealed in these analyses.

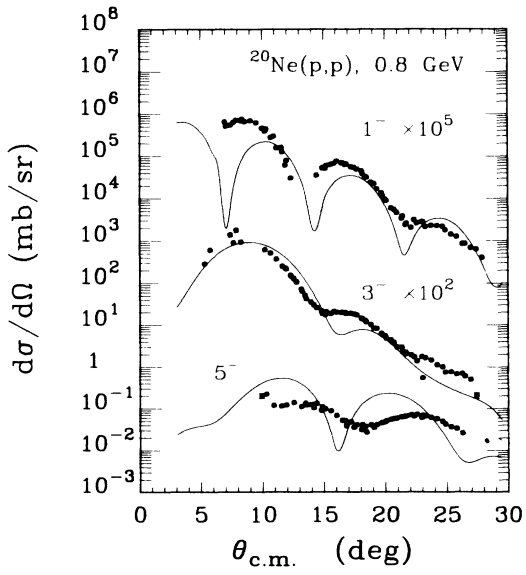

FIG. 4. The same as Fig. 3 for a $K^\pi=0^-$ octupole band.

IV. ^{22}Ne

The spins of the states of ^{22}Ne presented here were known from other works,[8] but the unique assignment of the levels to particular rotational bands had not been made previously. Presented here and shown in Figs. 5–7 are calculations for the GSRB, and for two possible side bands: a $K^\pi=2^+$ and $K^\pi=2^-$.

A. GSRB

The results of CC calculations are compared with the experimental results for the (ground state, 0^+) ($1.27,2^+$), and ($3.36,4^+$) states in Fig. 5. The known ($6.31,6^+$) state is masked by the ($6.34,4^+$) state. The Woods-Saxon potential parameters (V, W, r, a, r_c, β_2, and β_4) are (-12 and $+46.2$ MeV, 1.053, 0.46, and 1.05 fm, $+0.47$ and 0.10). β_6 has been taken to be 0.0 ± 0.05, which is a larger range than observed for other 6^+ states in this mass region. This range in β_6 has no effect on the 0^+ and 2^+ calculated angular distributions and, as seen in Fig. 5, the variations in the 4^+ calculations are small.

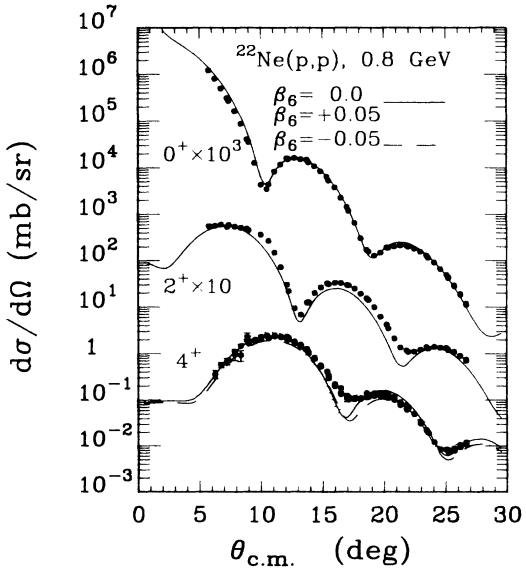

FIG. 5. Angular distributions of ^{22}Ne(p,p') for the 0^+, 2^+, and 4^+ states are shown. The curves result from CC calculations as discussed in the text.

B. $K^\pi=2^+$ bands

The possible $K^\pi=2^+$, γ-vibrational band considered here includes the $(4.46,2^+)$, $(5.6,3^+)$ (not observed), and $(6.34,4^+)$ states; the results are presented in Fig. 6. Shell-model calculations predict that the $(5.52,4^+)$ and the $(6.34,4^+)$ states have approximately equal neutron matrix elements with the ground state, while the proton matrix element for the $(5.52,4^+)$ state is 30% smaller than that for the $(6.34,4^+)$ state. Thus the $B(E4)$ for the $(6.34,4^+)$ state is predicted to be twice that for the $(5.52,4^+)$ state.[18] The $(5.52,4^+)$ decays primarily by an $M1$ transition to the $(3.36,4^+)$ state.[8] Calculations for the $(5.52,4^+)$ are not considered here, but data for its excitation are included in Ref. 9.

In previous analyses of $K^\pi=2^+$ bands in ^{24,26}Mg, satisfactory CC calculations required both an α_{22} $(Y_{22}+Y_{2-2})$ term, which directly excites the 2^+ member of the γ band, and an α_{42} $(Y_{42}+Y_{4-2})$ coupling which permits a strong direct transition from the ground state to the 4^+ state of the γ band.[6,12] The direct excitation which results from $Y_{20}\times Y_{22}$ terms in the multipole expansion of the deformation has been found to be more than an order of magnitude too small. The matrix elements utilized, η_1 and η_2, are defined in Ref. 4. Basically, $\eta_1 R$ is the matrix element of the vibrational operator α_{22}, which connects intrinsic states of the ground band to that of the γ band, and is approximately equal to $\beta_2\gamma R$. The matrix element $\eta_2 R$ is similarly related to the α_{42} coupling. In fitting the inelastic angular distributions, the matrix elements η_1 and η_2 were varied (including the relative sign) to produce the best overall agreement in magnitude for the 2^+ and 4^+ states.

The CC calculations for the possible γ band shown in Fig. 6 utilize $\eta_1 R=0.25$ fm and $\eta_2 R=0.47$ fm. The fit to the 2^+_γ state is not as good as in the case of similar calculations for ^{24}Mg and ^{26}Mg.[6] Due to the poor fit for the 2^+_γ, it is not possible to make a definite band assignment for these states. In comparing the strength of the coupling $(\eta_1 R)^2$ in ^{22}Ne and the Mg study, it is found that the ^{22}Ne strength is 50% of that in ^{24,26}Mg, and the ratio of the peak cross sections for the $2^+_\gamma/2^+_1$ is smaller than in the magnesium isotopes. It is interesting to note that this ratio of cross sections is smaller than that for the first two 2^+ states in ^{34}S. For ^{34}S, it has been suggested that the one-step amplitude for the second 2^+ state is suppressed, possibly due to a negative relative sign between neutron and proton transition elements.[13] Both of the second 2^+ states in ^{22}Ne and ^{34}S have shapes different than that predicted by a collective model DWBA calculation. The points at $\theta<9°$ for the $(6.34,4^+)$ are probably a contaminant, possibly the $(6.24,0^+)$, or due to the target windows which are present at angles below about 10°, and were not considered in the present analysis.

C. $K^\pi=2^-$ octupole band

Displayed in Fig. 7 are the results of a CC calculation similar to that already discussed for ^{20}Ne for a $K^\pi=2^-$. The GSRB is coupled to the $(5.15,2^-)$, $(5.91,3^-)$, and an unobserved 5^- state with $\alpha_{32}R=0.85$ fm. The strength of the coupling $(\alpha_{32}R)^2$ is 40% of that in ^{20}Ne. As for the analogous states in ^{20}Ne, the strength and slope of the angular distributions for both ^{22}Ne states are explained by the calculations. The agreement between the calculation and the data strongly suggests that the population of the 2^- state is dominated by multistep transitions.

V. MULTIPOLE MOMENTS

The extracted multipole moments of the imaginary part of the optical potential for ^{20}Ne and ^{22}Ne are given

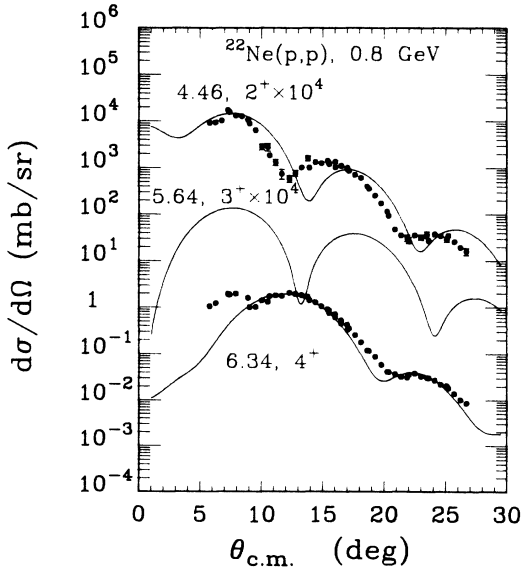

FIG. 6. Experimental angular distributions for states in ^{22}Ne assumed to comprise a $K^\pi=2^+$ γ-vibrational band.

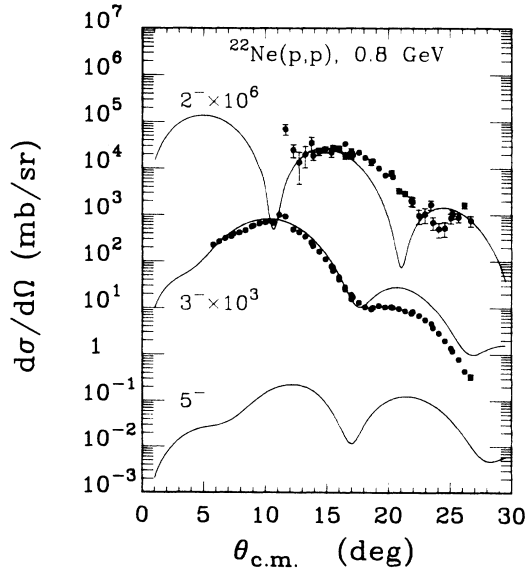

FIG. 7. Experimental angular distributions and CC calculation for negative-parity states in ^{22}Ne thought to comprise a $K^\pi=2^-$ band.

in Table I, along with results from electromagnetic studies,[14–18] low-energy proton scattering,[19–21] light-ion scattering,[22,23] and shell-model results.[24,25] Also given are proton and neutron matrix elements determined from pion inelastic scattering data.[26] The $M(E2)$ for ^{20}Ne is slightly smaller than the observed $B(E2)$ values while that for ^{22}Ne is in good agreement. Another analysis of this data which employed a deformed spin-orbit potential and utilized a χ-squared fit to the data is listed in Table I. The analysis reported here matches the calculation to the data near the first maximum.

Because the proton matrix element coupling the first 4^+ state to the ground state is predicted to be four times larger than the neutron matrix element,[25] the value of $M(E4)$ for this state is expected to be strongly dependent on the probe and on the incident energy. The strength for α scattering is expected to be 38% of the electromagnetic $B(E4)$. Using the relative interaction strengths for 800-MeV protons,[6] one would expect 44% of the electromagnetic $B(E4)$ if multistep effects are ignored. If such a difference alone resulted in a change in strength for the 4^+, this would imply that $\beta_4=0.15$ for electromagnetic probes and would result in $B(E4)=0.0160$ $e\,b^2$. The (e,e') result[18] is 0.013 ± 0.0015, which implies $Mn\approx Mp$. Using the relative interaction strengths for 30-MeV protons, one would expect 23% of the electromagnetic $B(E4)$, or one-half of the 800 MeV result. As seen in Table I, the $M(E4)$ for 30-MeV protons is slightly larger than that for 800-MeV protons. The β_4R value at 30 MeV is one-half of that for 800-MeV protons. Since the excitation of the 4^+ state in these calculations results from direct contributions from terms with β_4Y_4 and $(\beta_2Y_2)^2$ as well as multistep contributions, comparisons of β_4R may be misleading. The β_2R values are fairly uniform, and over half of the $M(E4)$ results from the β_2 term in the deformation. A coupled-channels analysis of pion inelastic scattering may be able to determine the nature of this state and its couplings to other members of the ground-state band.

In order to make comparisons for the excited states not in the GSRB between the current study and other work, a DWBA analysis of these states has been performed. The potentials obtained by fitting the elastic angular distributions are $(V, W, V_{so}, W_{so}, r, a, r_{so}, a_{so}, r_c)=(-1.0,$ 59.3, 0.775, and 2.02 MeV, and 0.949, 0.688, 0.954, 0.662, and 1.05 fm) for ^{20}Ne and (−3.9, 49.1, 0.775, and 2.02 MeV, and 1.016, 0.594, 0.994, 0.662, and 1.05 fm) for ^{22}Ne. The spin-orbit potential for ^{22}Ne was set equal to that determined for ^{20}Ne$(\vec{p},p)$ elastic scattering. The deformation parameters were obtained by fitting the first maximum of the predicted angular distribution to the data at that angle. The values of β_LR and computed $M(EL)$ values for each deformation are given in Table II. Also included are results from low-energy (p,p'),[21,27]

TABLE I. Multipole moments ($e\,b^{\lambda/2}$) and deformation lengths (fm).

Nucleus	$M(E2)$	$M(E4)$	β_2R	β_4R	Reaction	Reference
^{20}Ne	+0.162(3)[a]	+0.0223(14)	1.32	0.78	(p,p'), 800 MeV	This work
	+0.164	+0.0253	1.29	0.69	(p,p'), 800 MeV	b
	+0.179(7)				Coulomb	14
	+0.180	+0.023			Coulomb	15
	+0.171				Average electromagnetic	16
	0.189	0.027	1.47	0.87	(e,e')	17
	+0.181	+0.037	1.29	0.77	(p,p'), 30 MeV	19
	0.181	+0.037	1.29	0.77	(p,p'), 24.5 MeV	20
	0.214	0.041	1.47	0.53	(^{3}He,^{3}He'), 68 MeV	22
	0.178(7)	0.030(2)	1.30	0.41	(^{4}He,^{4}He'), 104 MeV	23
	0.179	0.034	1.29	0.68	(p,p'), 40 MeV	21
	0.150	0.0205			Shell model	24
^{22}Ne	+0.150(2)[a]	+0.0125(18)	1.39	0.29	(p,p'), 800 MeV	This work
	+0.132	+0.0109	1.12	0.27	(p,p'), 800 MeV	b
	+0.149(2)[d]				Coulomb	14
	+0.144	(−0.003)[c]			Coulomb	15
	+0.151(3)				Average electromagnetic	16
	0.165(11)	+0.013(2)			(e,e')	18
	+0.169	+0.014	1.38	0.15	(p,p'), 30 MeV	19
	+0.169	+0.014	1.38	0.15	(p,p'), 24.5 MeV	20
	+0.160(7)	+0.011(4)	1.25	0.07	(^{4}He, ^{4}He), 104 MeV	23
	+0.176	0.018	1.40	0.25	(p,p'), 40 MeV	21
	$Mn=0.176$, $Mp=0.152$	0.0117[c]			Shell model	24
	$Mn=0.187(13)$, $Mp=0.152(10)$				(π,π)	26

[a]These errors reflect only the uncertainty in β_6 as discussed in the text.
[b]Analysis of the same data reported here, employing a deformed spin-orbit potential in the CC calculations.
[c]Coupled-channels analysis of heavy-ion data just above the Coulomb barrier. The 4^+ state is not included in the analysis.
[d]Average of three measurements of the lifetime.
[e]$Mp=-0.0117$, $Mn=-0.0030$ (Ref. 25).

TABLE II. Deformation parameters of states in ^{20}Ne and ^{22}Ne.

	$B_L R$ (fm), $[M(EL)]$ (e fm^L)					
	(p,p')			(d,d')		
	800 MeV[a]	24 MeV[b]	40 MeV[c]	52 MeV[d]	(e,e')	Theory
^{20}Ne						
5.62,3$^-$	1.07,[46]	1.18,[58]	1.11(22),[56]	0.92,[54]	[42][e]	
7.17,3$^-$	0.76,[32]	0.82,[40]		0.95,[56]		
8.45,5$^-$	0.13,[150]					
^{22}Ne						
4.46,2$^+$	0.26,[2.4]				[3.6(3)][f]	[$Mp=-4.5, Mn=-0.7$][g]
5.52,4$^+$	0.28,[51]					[$Mp=72, Mn=106.0$][h]
5.91,3$^-$	0.68,[26]		0.73(5),[38]		[29.(4)][f]	
6.12,2$^+$	0.24,[2.3]				[1.8(4)][f]	[$Mp=+0.2, Mn=3.6$][g]
6.34,4$^+$	0.46,[84]					[$Mp=104., Mn=113.$][h]
7.94,2$^+$	0.15,[1.4]					[$Mp=+1.1, Mn=-0.6$][g]

[a]This work.
[b]Reference 27.
[c]Reference 21.
[d]Reference 28.
[e]Reference 29.
[f]Reference 18.
[g]Reference 24.
[h]Reference 25.

(d,d'),[28] (e,e'),[18,29] and shell-model results.[24,25] One general feature is that the $\beta_L R$ values are in agreement. The $M(EL)$ for low-energy proton and deuteron inelastic scattering are higher than those for 800 MeV (p,p') and (e,e'). It is well established that the moments of the potential are closely related to the moments of the nuclear density at 800 MeV, while a complicated folding of the low-energy interaction with the nuclear density is required to yield low-energy microscopic potentials. The differences between the $M(EL)$ values for states in ^{22}Ne excited by (p,p') and (e,e') may reflect a difference in Mp and Mn for these states. Pion inelastic scattering data would be useful for these states as well.

VI. SUMMARY AND CONCLUSIONS

Measurements of the angular distributions for 0.8-GeV proton elastic and inelastic scattering to many excited states in ^{20}Ne and ^{22}Ne have been presented. Coupled-channels calculations based on the collective rotational model provide excellent descriptions of the data for the ground-state rotational bands. In both isotopes, negative-parity states assigned to a $K^\pi=2^-$ band are well explained by pure direct transitions to the 3^- states and multistep excitation of observed 2^- members in ^{20}Ne and ^{22}Ne.

The assignment of the $(8.45,5^-)$ state to the $K^\pi=2^-$ band is not certain, as the data can also be explained as belonging to a $K^\pi=0^-$ band. Similarly, no band assignment can be made for the second 2^+ state in ^{22}Ne, since it is poorly described by the CC calculations explained with calculations assuming it to belong in a γ-vibrational band with the third of the 4^+ states. Deformation parameters and multipole moments of the empirical, deformed optical potentials are similar to results obtained with other probes. Data on resonance pion scattering would be useful to verify the shell-model neutron and proton matrix elements for the states in ^{22}Ne.

ACKNOWLEDGMENTS

The authors would like to thank the LAMPF staff for their assistance in performing these measurements, and especially Bob Damjonovich for his assistance in the construction of the gas target. The research reported here was supported in part by the U.S. National Science Foundation, the U.S. Department of Energy, and the Robert A. Welch Foundation.

*Present address: Arizona State University, Tempe, AZ 85287.
†Present address: Rutgers University, New Brunswick, NJ 08903.
‡Present address: Los Alamos National Laboratory, Los Alamos, NM 87545.

[1]L. Ray, G. S. Blanpied, W. R. Coker, R. P. Liljestrand, and G. W. Hoffmann, Phys. Rev. Lett. **40**, 1547 (1978).
[2]G. S. Blanpied *et al.*, Phys. Rev. C **23**, 2599 (1981).
[3]G. S. Blanpied *et al.*, Phys. Rev. C **20**, 1490 (1979).
[4]L. Ray, G. S. Blanpied, and W. R. Coker, Phys. Rev. C **20**, 1236 (1979).
[5]M. L. Barlett *et al.*, Phys. Rev. C **22**, 1168 (1980).
[6]G. S. Blanpied *et al.*, Phys. Rev. C **25**, 422 (1982).
[7]G. S. Blanpied *et al.*, Phys. Rev. C **30**, 1233 (1984).
[8]X. K. Maruyama *et al.*, Phys. Rev. C **19**, 1624 (1979); P. M. Endt, At. Data Nucl. Data Tables **23**, 3 (1979).
[9]See AIP document No. PAPS PRVCA 38-2180-81 for 81 pages of numerical data for elastic and inelastic scattering of 0.8-GeV protons from ^{20}Ne and ^{22}Ne. Order by PAPS number and journal reference from American Institute of Physics,

Physics Auxiliary Publication Service, 335 East 45th Street, New York, NY 10017. The price is $1.50 for microfiche or $12.65 for photocopied. Airmail additional. Make checks payable to the American Institute of Physics.

[10]T. Tamura, Rev. Mod. Phys. **37**, 679 (1965); T. Tamura, Oak Ridge National Laboratory Report No. ORNL-4152, 1967.

[11]L. W. Put and M. N. Harakeh, Phys. Lett. **119B**, 253 (1982).

[12]K. Van der Borg, M. N. Harakeh, and B. S. Nilsson, Nucl. Phys. **A325**, 31 (1979).

[13]A. M. Bernstein *et al.*, Phys. Rev. Lett. **49**, 455 (1982).

[14]D. Schwalm, E. K. Warburton, and J. W. Olness, Nucl. Phys. **A293**, 425 (1977).

[15]E. E. Gross *et al.*, Phys. Rev. C **29**, 459 (1984).

[16]B. H. Wildenthal, in *Elementary Modes of Excitation in Nuclei,* edited by A. Bohr and R. A. Broglia (North-Holland, Amsterdam, 1977), p. 383.

[17]Yataro Horikawa, Akira Nakada, and Yoshihru Torizuka, Prog. Theor. Phys. **49**, 2005 (1973).

[18]X. K. Maruyama *et al.*, Phys. Rev. C **19**. 1624 (1979).

[19]R. de Swiniarski, F. G. Resmini, D. L. Hendrie, and A. D. Bacher, Nucl. Phys. **A261**, 111 (1976).

[20]R. de Swiniarski *et al.*, Phys. Rev. Lett. **17**, 1139 (1972).

[21]D. Madland, Ph.D. thesis, University of Minnesota, 1970 (unpublished).

[22]R. de Swiniarski *et al.*, Lett. J. Phys. L **35**, 425 (1974).

[23]H. Rebel *et al.*, Nucl. Phys. **A182**, 145 (1972).

[24]B. A. Brown, R. Radhi, and B. H. Wildenthal, Phys. Rep. **101**, 314 (1983).

[25]B. H. Wildenthal, B. A. Brown, and I. Sick, Phys. Rev. C **32**, 2185 (1985); B. A. Brown, W. Chung, B. H. Wildenthal, *ibid.* **21**, 2600 (1980).

[26]C. L. Morris *et al.*, Phys. Rev. C **35**, 1388 (1987).

[27]R. de Swiniarski *et al.*, Helv. Phys. Acta **49**, 241 (1976).

[28]F. Hinterberger *et al.*, Nucl. Phys. **A115**, 570 (1968).

[29]D. Hausser *et al.*, Nucl. Phys. **A168**, 17 (1971).